RSC Advances

This article can be cited before page numbers have been issued, to do this please use: Y. Yan, S. Jiang and H. Zhang, *RSC Adv.*, 2015, DOI: 10.1039/C5RA19832A.

ROYAL SOCIETY OF CHEMISTRY

www.rsc.org/advances

View Article Online
DOI: 10.1039/C5RA19832A

Catalytic wet oxidation of phenol with Fe-ZSM-5 catalysts

Ying Yan, Songshan Jiang, Huiping Zhang*

School of Chemistry and Chemical Engineering, South China University of Technology, Guangzhou 510640, PR China

Abstract: Fe-ZSM-5 and Fe_2O_3/ZSM-5 zeolite catalysts were prepared and tested for catalytic wet oxidation of phenol. Firstly, Fe-ZSM-5 and Fe_2O_3/ZSM-5 zeolite catalysts were prepared by hydrothermal synthetic and incipient wetness impregnation and characterized to determine the framework and extraframework Fe^{3+} species. Secondly, catalytic properties of Fe-ZSM-5 in the oxidation of phenol were systematically studied to determine the optimum technological parameters by investigating the effects of reaction temperature, pH, catalyst concentration and stirring rate on the conversion of phenol. Besides, the phenol conversion, selectivity to CO_2 and concentration of aromatics intermediates in the oxidation of phenol with two catalysts were analyzed under the same optimum conditions. Leaching of iron from the catalysts as well as the catalytic stability of Fe-ZSM-5 was also tested. Finally, the kinetics of catalytic wet oxidation of phenol with Fe-ZSM-5 was studied. The experimental results showed that both the framework and extraframework Fe^{3+} species were together present in the Fe-ZSM-5. The oxidation reaction with Fe-ZSM-5 was performed well at temperature of 70℃，pH of 4, catalyst concentration of 2.5 g/L and stirring rate of 400 rpm, reaction time of 180 min and the conversion of phenol reached 94.1%. From the catalytic results of two catalysts, it can be concluded that framework Fe^{3+} species may be more efficient in the phenol oxidation than extraframework Fe^{3+} species, a better stability of Fe-ZSM-5 and a relative low decrease of activity could be found after three consecutive runs. Activation energy of 27.42 kJ/mol was obtained for phenol oxidation with Fe-ZSM-5.

Keywords: Fe-ZSM-5; Phenol; Catalytic wet oxidation; Framework Fe

* Corresponding author: Tel: +86 2087111975; fax: +86 2087111975.
E-mail address: hpzhang@scut.edu.cn (H.P. Zhang).

View Article Online
DOI: 10.1039/C5RA19832A

1. Introduction

Phenol is a typical pollutant from industry, especially appears in wastewaters form refineries, petrochemical, pharmaceutical and so on[1, 2]. How to efficiently eliminate phenol from water and wastewater is still focused by many researchers today.

A various techniques such as biological, physical and chemical treatments have been used to purify these industrial organic wastewaters[3-5]. However, conventional biological method is not widely used to treat highly non-biodegradable wastewater and also requires too long residence time for micro-organisms to degrade the pollutants[6]. Physical treatments, for example, adsorptive processes，which are useful in the purification of diluted wastewaters need a further destructive post-treatment[7]. Advanced oxidation processes are much more effective in decomposing a wide range of organic pollutants, especially for the high concentration phenolic wastewater (> 1000 mg/L) among the chemical treatment technologies[8]. There are a lot of different available oxidants like ozone, oxygen, hydrogen peroxide as well as some combinations, such as H_2O_2/UV, H_2O_2/O_2 can be used in advanced oxidation processes. Catalytic wet peroxide oxidation based on the Fenton-type process is considered as a relative lower cost and higher efficiency process for organic pollutants[9], however, the use of metallic salts as catalysts are precipitated as $Fe(OH)_3$ which results in an additional pollution. In order to avoid additional pollution, heterogeneous catalysis is a good choice to minimize the concentration of transition metal ions generated during the reaction, and these heterogeneous catalysts are always in the form of active iron over the supports[10]. Zeolites as the porous materials have been widely used as the effective catalyst supports in the environment, industries and other important areas[11-13]. Recent works have demonstrated to prepare a series of Fe-bearing solid catalysts like iron-supported meso-structured silica supports[14, 15], activated carbon impregnated with iron[16], iron modified zeolites[17, 18], and other iron catalysts[19] used in catalytic wet peroxide oxidation of phenolic wastewater. Among these iron catalysts, Fe-ZSM-5 as a heterogeneous catalyst earlier used in NO_x reduction[20] and catalytic wet peroxide oxidation of phenol wastewater were studied on the synthesis and catalytic activity in some literatures[21, 22], including synthesis process, catalytic activity and deactivation. Although Fe-ZSM-5 as the catalyst has been studied in the oxidation of phenol recent years, to the best of our knowledge, there are not so many works on the systematical research of catalytic wet oxidation of phenol with Fe-ZSM-5.

View Article Online
DOI: 10.1039/C5RA19832A

The purpose of this work is to study the catalytic properties of framework and extraframework Fe^{3+} species in two types of iron zeolites catalyst for the catalytic wet oxidation of phenol with H_2O_2 as the oxidant. In addition, a systematical work on characterization, technological parameters, selectivity to CO_2, aromatics intermediates, stability and activation energy will be presented in this paper.

2. Experimental

2.1 Materials

Phenol was purchased from Guangzhou Chemical Reagent Factory. Hydrogen peroxide (H_2O_2, 30wt. % aqueous) was purchased from Shanghai Qiangshun Chemical Reagent Factory. Tetrapropylammonium hydroxide (TPAOH) was purchased from Tianjin Guangfu Fine Chemical Research Institute. Tetraethoxysilane (TEOS) was purchased from Tianjin Fuchen Chemical Reagent Factory. Sodium aluminate ($NaAlO_2$) was purchased from Sinopharm Chemical Reagent Co., Ltd. $Fe(NO_3)_3 \cdot 9H_2O$ was purchased from Tianjin Damao Chemical Reagent Factory. ZSM-5 zeolites (Si/Al=50) with average particle diameter of 1mm were purchased from Nankai University Catalyst Factory. Catechol, hydroquinone, resorcinol and benzoquinone purchased from Sinopharm Chemical Reagent Co., Ltd. were all used as standard samples for the test. Deionized water was used in all synthesis process. All of the chemical reagents used in this study were analytical grade.

2.2 Preparation of Fe-ZSM-5 Catalysts

Fe-ZSM-5 zeolite catalyst was synthesized by hydrothermal synthesis from a mixture solution with the molar ratio: $5000H_2O$:100TEOS:10TPAOH:$2NaAlO_2$:2 $Fe(NO_3)_3 \cdot 9H_2O$. The mixture solution was aged 24 h and treated hydrothermally in a 50 ml Teflon lined autoclave at 170 ℃ for 48 h. The resulting white solid was filtered, ultrasonic washed by deionized water for 20 min and dried at 100 ℃, then calcined at 550 ℃ in airflow for 4 h.

Fe_2O_3/ZSM-5 zeolite catalyst was prepared by incipient wetness impregnation method, involving the impregnation of ZSM-5 with proper amount of $Fe(NO_3)_3 \cdot 9H_2O$. After impregnation, the catalyst was dried at 110 ℃ for 24 h, then calcined at 550 ℃ in airflow for 8 h. The Fe load was adjusted to 1.5 wt. % in both two prepared catalysts.

View Article Online
DOI: 10.1039/C5RA19832A

2.3 Catalyst characterization

Different techniques were used for the characterization of the catalysts. X-ray diffraction (XRD) using a D8 ADVANCE (Bruker Co.) diffractometer with Cu Kα radiation (40 kV, 40 mA) with 2θ range of 5–60° was used to determine the crystalline phases present in both the catalysts and support. The structure properties of the catalysts were analyzed by a Fourier transform infrared (FTIR, Spectnlm2000, Perkin Elmer, USA) with a resolution of 4 cm-1 in the range from 400 - 4000 cm-1 at a room temperature. A typical pellet containing 1 wt% of sample was prepared by mixing 1 mg sample with 100 mg KBr. Temperature programmed reduction (TPR) tests were performed on Quantachrom Automated Chemisorption Analyzer in a flowing H_2 reduction system with a TCD detector. A 50mg of each sample was loaded into the reactor and purged with 50ml/min of Ar at 350 ℃ for 30 min to eliminate contaminants, and then cooled down to 50 ℃. The temperature was increased to 900 ℃ at a heating rate of 10 ℃/min with flowing of 10% H_2 and 90% Ar. The structure modification involving Fe^{3+} species were identified by UV-vis reflectance spectra carried out on a UV spectrophotometer (U-3010, Hitachi, Japan) in the 200-700 nm wavelength range employing $BaSO_4$ as blank.

2.4 Catalytic wet oxidation of phenol

The oxidation of phenol was carried out in batch in 250 mL stoppered glass flask in a water bath with a condenser, thermocouple and pH electrode at a certain stirring rate. A volume of 200 mL of a 2500 mg/L phenol aqueous solution and a certain weight of Fe-ZSM-5 zeolite catalyst were transferred into the flask. The experiments were carried out at different temperatures of 40-80 ℃, pH=2-6 and stirring rate of 200-600 rpm. The H_2O_2 : phenol molar ratio was fixed at 21 for complete oxidation of phenol up to CO_2 and H_2O, whereas the stoichiometric ratio is 14. The amount of H_2O_2 used was in excess, which was equal to 1.5 times of the H_2O_2 amount necessary to completely oxidate phenol to CO_2 and H_2O. When the reaction temperature was reached, H_2O_2 was dropped into the flask, and the reaction was then considered to start. In addition, the effects of different catalyst loads (0.5-5 g/L) were also tested in these experiments.

Liquid samples were taken at different time intervals and immediately analyzed. The concentration of phenol and identification of intermediates were carried out in a HPLC (model 1100, Agilent Technologies, USA) with a HC-C18 reverse phase column (5 μm×250 mm×4.6 mm). Total organic

View Article Online
DOI: 10.1039/C5RA19832A

carbon (TOC) values were obtained by a TOC Analyser (Sievers Innov, General Electric, USA).

The calculation method given by Nguyen et al.[23] was applied to determine the conversion of phenol (X_{phenol}, %) and selectivity to carbon dioxide (S_{CO2}, %).

2.5 Stability tests

Leaching tests were carried out to investigate whether small amounts of the dissolved iron were responsible for the observed catalytic activity. The ion contents of the reaction solution were measured at different time intervals by atomic adsorption spectroscopy (AA240FS, Varian, USA).

Three consecutive runs were conducted with the same Fe-ZSM-5 zeolite catalyst load at 70 ℃ and pH of 4 after simply drying at 100 ℃. The conversion of phenol was tested at different time intervals in order to analyze the stability of the zeolite catalyst.

3. Results and discussion

3.1 Characterization of Catalysts

To confirm the structure and the crystallinity, different samples were analyzed by using XRD. The XRD patterns of ZSM-5, Fe_2O_3/ZSM-5 and Fe-ZSM-5 are shown in Fig.1. In the XRD patterns, all the samples give the same diffraction peaks at the ranges of 2θ=7–9° and 2θ=23–25°, which matching well with the reports on MFI-structure[24]. It is known that metal-impregnation thus affects the structure regularity of zeolites found by other researchers[17, 25, 26]. As we can see in the XRD patterns of Fe-ZSM-5, the higher intensities of diffraction peaks appear at 2θ=7–9°, comparing with other two samples, which suggests that Fe^{3+} may be successfully incorporated into the MFI framework[27]. In addition, in the XRD patterns of Fe-ZSM-5 and Fe_2O_3/ZSM-5, there are two weak diffraction peaks of α-Fe_2O_3 at 2θ=33° and 36°, which infers for isolated extraframework Fe^{3+} species in both Fe-ZSM-5 and Fe_2O_3/ZSM-5. The intensity decrease of the XRD patterns at 2θ=23–25° of the Fe-ZSM-5 and Fe_2O_3/ZSM-5 could also confirm the existence of Fe species.

Infrared spectroscopy is a tool widely used to characterize the structural properties of zeolites. Useful information can be obtained by exploring the framework (1350-400 cm^{-1}) regions[28]. The IR spectra of ZSM-5, Fe_2O_3/ZSM-5 and Fe-ZSM-5 are shown in Fig.2. IR spectra of all the samples shows that same absorption peaks centred at 1225 cm^{-1}, 1093 cm^{-1}, 790 cm^{-1}, 550 cm^{-1} and 450 cm^{-1}, matching with

View Article Online
DOI: 10.1039/C5RA19832A

skeletal vibrations of MFI zeolite structure (ZSM-5). The bands at 550 cm^{-1} is assigned to the vibration of double 5-rings in MFI lattice and the ratio of band intensities at 500 and 450 cm^{-1} is often used as an indication of zeolite crystallinity[23]. From the IR spectra of Fe-ZSM-5, there is an absorption peak centered at 980 cm^{-1}. The absorption peak centered at 960 cm^{-1} is considered as the vibrations of $SiO^{\delta-}\cdots Tx^{\delta+}$, where $Tx^{\delta+}$ is the heteroatom located into the framework [29]. In some reports[30], the bands around 1000 cm^{-1} can be explained that the local structure surrounding the framework Fe^{3+} species is described by 4 $[O_3Si\text{-}O]^-$ units, which can be also used to support the framework Fe^{3+} species present in Fe-ZSM-5.

Temperature-programmed reduction (TPR) experiments were carried out to get further study into iron species and their redox properties[30, 31]. The TPR curves of ZSM-5 and Fe-ZSM-5 are shown in Fig. 3.The TPR curve of Fe-ZSM-5 shows a clearly maxima centered at 843 ℃. The peak observed at this temperature can be ascribed to a residual fraction of framework Fe^{3+} species of difficult reducibility, because the reduction of framework Fe^{3+} species usually occurs at a temperature higher than 677 ℃[32]. Moreover, as we can see in the TPR curve of Fe-ZSM-5, there is a weak signal peak at 353 ℃, compared with the TPR curve of ZSM-5. It has been proposed that the iron mostly in the form of Fe_2O_3 on the surface of Fe-ZSM-5 and reduced from Fe^{3+} to Fe^{2+} at around 400 ℃[33].

UV-vis spectroscopy is applied to analyze the structural modification involving Fe^{3+} species[30]. The UV-vis reflectance spectrum of Fe-ZSM-5 is shown in Fig. 4. Two strong absorption peaks appeared between 200 nm and 300 nm with ligand to metal Fe^{3+} charge transfer character involving isolated framework Fe^{3+}. Meanwhile, the appearance of a weak broad absorption centered at 380 nm. It can be ascribed to Fe^{3+} species present in the form of Fe_2O_3 particles.

From these results, it could be concluded that both the framework and extraframework Fe^{3+} species are together present in the Fe-ZSM-5, but only extraframework Fe^{3+} species in the Fe_2O_3/ZSM-5 prepared by incipient wetness impregnation.

3.2 Phenol Oxidation with Fe-ZSM-5

3.2.1 Effects of reaction temperature

The reaction temperature is one of the most important parameters in the oxidation of phenol. The conversion of phenol was tested over different temperatures from 40 ℃ to 80 ℃, and the results are shown in Fig. 5. As can be seen in Fig.5, an increase in reaction temperature up to 80 ℃ results in the

View Article Online
DOI: 10.1039/C5RA19832A

enhancement of the conversion of phenol from 65.6% to 95.9%. Similar observations had been reported for other iron containing catalysts[34, 35]. An increase of temperature results in higher H_2O_2 decomposition into HO • radicals leading to higher phenol conversion[10]. However, high reaction temperature can result in a degradation of H_2O_2 into H_2O and O_2. Thus, in this study, a reaction temperature of 70 ℃ was chosen as the optimum reaction temperature, because the conversion of phenol can also come to 94.1% at this temperature and there is no significant enhancement (95.9%) at temperature of 80 ℃.

3.2.2 Effects of pH

Eisenhauer[36] concluded that a pH of 3-4 was the optimum value for phenol oxidation by H_2O_2 with iron as the catalyst. In order to investigate the optimum initial pH in the oxidation of phenol, the conversion of phenol was tested over different acidity (pH = 2-6), and the results are shown in Fig. 6. As we can see in Fig. 6 (a), the conversion of phenol remarkably rises with decreasing acidity. Meanwhile, the rate of conversion of phenol increases rapidly as reaction time increases to 60 min but reduces in the further increase of time to 180 min. It is also known form Fig. 6 (b) that initial pH of 4 is clearly the advisable operating value in the oxidation of phenol. One possible reason is that the leaching of iron cations is enhanced at low pH values[21]. And another reason for the decrease of phenol conversion at pH 5 and 6 may be the decomposition of H_2O_2 into H_2O and O_2 which likely leaded to the accelerated formation of less reactive peroxy radicals (H_2O •) rather than HO • radicals[37]. A similar trend was obtained by Zazo[38] using Fe/activated carbon as catalyst in oxidation of phenol.

3.2.3 Effects of catalyst concentration

The influence of different catalyst concentration (0.5 g/L, 1.25 g/L, 2.5 g/L, 3.75 g/L and 5 g/L) on oxidation of phenol was investigated and the results are shown in Fig. 7. A significant increase in the conversion of phenol is observed as catalyst concentration increases. The conversion of phenol dramatically increases from 31.2% to 94.1% with the catalyst concentration increasing from 0.5 g/L to 2.5 g/L. however, the conversion of phenol rises slowly in further increase of catalyst concentration. High catalyst concentration (high Fe^{3+} content) can promote a higher H_2O_2 decomposition into HO • radicals. Here, Fe^{3+} content is different from the iron loading concentration in the catalysts. The report[39] on investigating the oxidation of phenol by using different iron loading (5 wt. %, 10 wt. %, 15 wt. % and 20 wt. %) in the catalyst concluded that high iron loading concentration could actually cause the pores

View Article Online
DOI: 10.1039/C5RA19832A

blocking which lead to less Fe^{3+} active sites deep within the catalyst matrix and lower the catalytic activity. Thus, more experiments will be performed with a series of iron loading in Fe-ZSM-5 in the future.

3.2.4 Effects of stirring rate

The conversion of phenol was tested at different stirring rate varying from 200 to 600 rpm, and the results are shown in Fig. 8. Obviously, the conversion of phenol increases from 75.1% to 94.1% with the stirring rate increasing from 200 rpm to 400 rpm. An increase in stirring rate results in violent collision between the molecules of solid and liquid, which lead to mass transfer enhancement in the oxidation of phenol. However, the conversion of phenol is not altered significantly in further increase of stirring rate from 400 rpm to 600 rpm.

3.3 Catalyst activity with framework Fe

In order to investigate the contribution of framework and extraframework Fe^{3+} species in the oxidation of phenol, the conversion of phenol and selectivity to CO_2 with Fe-ZSM-5 and Fe_2O_3/ ZSM-5 (1.5 wt. % Fe) under the same operating conditions (pH=4, *T*=70 ℃ and stirring rate =400rpm) were analyzed, respectively, and the results are shown in Fig. 9 and Fig. 10. It can be observed in Fig. 9 that the conversion of phenol over Fe_2O_3/ZSM-5 reaches 100% which is obviously higher than that over Fe-ZSM-5. In other words, the activity of extraframework Fe^{3+} species are higher than that of framework Fe^{3+} species, because extraframework Fe^{3+} species present in the form of iron oxide (Fe_2O_3) located in the pores as well as on the surface of zeolites, which indicates higher activity. However, as can be seen in Fig. 10, Fe-ZSM-5 shows a better selectivity to CO_2 (90.6%) compared with Fe_2O_3/ZSM-5 (only 77.6%) , which indicates that framework Fe^{3+} species can more efficiently catalyze to destroy phenol ring and convert it into CO_2 than extraframework Fe^{3+} species[23]. Two forms of Fe^{3+} species existed in the Fe-ZSM-5, namely, extraframework and framework Fe^{3+} species, but only extraframework Fe^{3+} species existed in the Fe_2O_3/ZSM-5. The extraframework Fe^{3+} species may have higher catalytic activity but lower stability. The higher activity of extraframework Fe^{3+} species will decompose the H_2O_2 into O_2 directly which resulted in lower CO_2 selectivity. However, the Fe-ZSM-5 catalyst can produce more •OH radicals by catalyzing H_2O_2 with higher utilization efficiency which resulted in higher CO_2 selectivity compared with Fe_2O_3/ZSM-5.

View Article Online
DOI: 10.1039/C5RA19832A

To learn more about the potential feasibility of framework and extraframework Fe^{3+} species in the oxidation of phenol, aromatics intermediates concentration in the oxidation with Fe-ZSM-5 and Fe_2O_3/ZSM-5 were tested to evaluate ecotoxicity during the oxidation process. HPLC was used to identify the aromatics intermediates, and the distribution curves of identified aromatics intermediates are shown in Fig. 11. It is known that the most likely pathway for oxidative destruction of phenol includes the primary products corresponding to aromatics resulting from phenol hydroxylation, and then evolving to simple carboxylic acids and finally completing oxidation to CO_2 and H_2O. From Fig. 11, four aromatics intermediates as well as TOC values were tested. It is found that lower aromatics intermediates concentration generate in the oxidation of phenol over Fe-ZSM-5 compared with that over Fe_2O_3/ZSM-5, which suggests relatively lower values of ecotoxicity in the oxidation of phenol over Fe-ZSM-5. However, the reaction time also plays a very important role in the oxidation, and it must reach sufficiently low concentrations of aromatics intermediates which are much more toxic than phenol itself[40]. In addition, the TOC reductions over these two zeolites catalysts after 180 min both come to at least 80%. The residual TOC is relative contributed by the simple carboxylic acids (which are more resistant to oxidation) evolved by the primary products from phenol ring opening and oxidation of the aromatics intermediates[41].

3.4 Stability and reusability of the catalysts

Leaching tests were also carried out over these two catalysts under the same reaction conditions to study much more about the stability of the catalysts in the oxidation process, and the results are shown in Fig. 12. It is observed that irons loading in the Fe-ZSM-5 and Fe_2O_3/ZSM-5 after leaching tests are 1.32 wt. % and 1.24 wt. %, respectively. Insignificant reduction in iron loading during the reaction indicates that two catalysts are not prone to much leaching, compared with the iron loading of 1.5 wt. % in fresh catalyst. But it is still found that a remarkable decrease of iron loading in the Fe_2O_3/ZSM-5, compared with that in Fe-ZSM-5.

From the results above, the reusability of Fe-ZSM-5 was carried out over three consecutive runs under the optimum reaction conditions, and the results are shown in Fig. 13. The conversion of phenol decreases from 94.1% at the 1st run to 85.6% at the 3rd run. Many reports[10, 42, 43] concluded that the decrease of catalyst activity cannot be attributed to Fe leaching from the catalyst. One important fact is the presence of residual carbon-containing matter over the surface of the used catalysts due to the absorption of

View Article Online
DOI: 10.1039/C5RA19832A

residual organic compounds onto the catalyst. Many methods such as washing by solvent, calcining at high temperature etc. are used to recover the catalyst, thus, more experiments will be performed in the future for a better understanding of catalyst regeneration.

3.5 Kinetics of catalytic wet oxidation of phenol with Fe-ZSM-5

A plot of initial rate of phenol (r_{A0}) vs. stirring rate was drawn in the range of 200-600 rpm for the external diffusion elimination, meanwhile, a plot of initial rate (r_{A0}) vs. particle size of Fe-ZSM-5 zeolite catalyst was also drawn in the range of 20-120 mesh for the internal diffusion elimination in this kinetic experiment under the optimum experimental conditions, and the results are shown in Fig. 14 and Fig. 15, respectively. It is easily to found that the external diffusion and internal diffusion are eliminated at the stirring rate of 400 rpm and particle size of 80 meshes.

The catalytic wet oxidation of phenol over Fe-ZSM-5 with excess H_2O_2 can be assumed to be a first-order reaction, and the reaction rate equation is:

$$-\frac{dC_A}{dt} = -r_{A0} = k_0 \exp(-\frac{E_a}{RT})C_A \qquad (1)$$

Where C_A is the phenol concentration at time t in mg/L, k_0 is pre-exponential factor in min^{-1}, E_a is the activation energy in kJ/mol, T is the reaction temperature in K.

The oxidation rates have been tested for first-order kinetics, by plotting $\ln(C_{A0}/C_A)$vs. time at different temperatures from 40 ℃ to 70 ℃, as shown in Fig. 16. The slopes of the straight lines were obtained and the values of the first-order rate coefficient are showed in table 1. These results confirm that the catalytic reactions usually follow first-order kinetics as the related investigation[25, 44].

Fig. 17 presents the Arrhenius plot of ln$k$ vs. $1/T$ obtained at different temperatures from 40 ℃ to 70 ℃. From the slope of Arrhenius plot in Fig. 17, the activation energy was calculated to be 27.42 kJ/mol. Consequently, initial oxidation rate can be expressed by the following equation:

$$-r_{A0} = 212.725e^{-27.42/RT}C_A \qquad (2)$$

Similar results of activation energy of wastewaters by catalytic wet oxidation were reported. For example, Xu et al.[45] calculated the activation energy which was 25.21 kJ/mol in the homogeneous catalytic Fenton oxidation of Reactive Brillant Blue X-BR azo dye.

4. Conclusions

View Article Online
DOI: 10.1039/C5RA19832A

Fe-ZSM-5 and Fe_2O_3/ZSM-5 zeolite catalysts with 1.5wt. % Fe for catalytic wet oxidation of phenol were prepared by hydrothermal synthetic and incipient wetness impregnation, respectively. Both the framework and extraframework Fe^{3+} species were together present in Fe-ZSM-5, but only extraframework Fe^{3+} species in Fe_2O_3/ZSM-5. The oxidation reaction with Fe-ZSM-5 was performed well at the atmospheric pressure, temperature of 70 ℃，pH of 4, catalyst concentration of 2.5 g/L and stirring rate of 400 rpm, reaction time of 180 min and the conversion of phenol reached 94.1%. Both the framework and extraframework Fe^{3+} species could catalyze the oxidation of phenol, however, framework Fe^{3+} species can be more efficient to oxidize phenol completely into CO_2. Fe-ZSM-5 zeolite catalyst showed a better stability than Fe_2O_3/ZSM-5, and a relative low decrease of activity after three consecutive runs. Reaction activation energy of oxidation with Fe-ZSM-5 zeolite catalyst was calculated as 27.42kJ/mol.

Acknowledgement

The authors gratefully acknowledge the financial support from the National Natural Science Foundation of China (Grant No. 21176086 and Grant No. 21006030) for this work.

References:

1. G. Busca, S. Berardinelli, C. Resini and L. Arrighi, *J. Hazard. Mater.*, 2008, **160**, 265-288.
2. P. Zhang, Y. Gong, H. Li, Z. Chen and Y. Wang, *RSC Advances*, 2013, **3**, 5121-5126.
3. S. Collado, A. Laca and M. Diaz, *J. Environ. Manage.*, 2012, **102**, 65-70.
4. N. Chaouati, A. Soualah and M. Chater, *Cr Chim.*, 2013, **16**, 222-228.
5. N. Inchaurrondo, P. Haure and J. Font, *Desalination*, 2013, **315**, 76-82.
6. N. S. Inchaurrondo, P. Massa, R. Fenoglio, J. Font and P. Haure, *Chem. Eng. J.*, 2012, **198**, 426-434.
7. P. R. Gogate and A. B. Pandit, *Adv. Environ. Res.*, 2004, **8**, 501-551.
8. J. Arana, E. T. Rendón, J. D. Rodrıguez, J. H. Melián, O. G. Dıaz and J. P. Pena, *Chemosphere*, 2001, **44**, 1017-1023.
9. E. G. Garrido-Ramirez, M. V. Sivaiah, J. Barrault, S. Valange, B. K. Theng, M. S. Ureta-Zañartu and M. de la Luz Mora, *Micropor. Mesopor. Mat.*, 2012, **162**, 189-198.
10. P. Bautista, A. F. Mohedano, N. Menendez, J. A. Casas and J. J. Rodriguez, *Catal. Today*, 2010, **151**, 148-152.
11. K. Jíša, J. Nováková, M. Schwarze, A. Vondrová, S. Sklenák and Z. Sobalik, *J. Catal.*, 2009, **262**, 27-34.

View Article Online
DOI: 10.1039/C5RA19832A

12. J. Pieterse, S. Booneveld and R. W. Van den Brink, *Appl. Catal. B: Environ.*, 2004, **51**, 215-228.
13. S. Jiang, H. Zhang and Y. Yan, *Catal. Comm.*, 2015, **71**, 28-31.
14. G. Satishkumar, M. V. Landau, T. Buzaglo, L. Frimet, M. Ferentz, R. Vidruk, F. Wagner, Y. Gal and M Herskowitz, *Appl. Catal. B: Environ.*, 2013, **138**, 276-284.
15. L. Xiang, S. Royer, H. Zhang, J. Tatibouët, J. Barrault and S. Valange, *J. Hazard. Mater.*, 2009, **172**, 1175-1184.
16. C. Chiu, K. Hristovski, S. Huling and P. Westerhoff, *Water Res.*, 2013, **47**, 1596-1603.
17. F. Adam, J. Wong and E. Ng, *Chem. Eng. J.*, 2013, **214**, 63-67.
18. H. Kušić, N. Koprivanac and I. Selanec, *Chemosphere*, 2006, **65**, 65-73.
19. J. Faye, E. Guélou, J. Barrault, J. M. Tatibouët and S. Valange, *Top. Catal.*, 2009, **52**, 1211-1219.
20. H. Chen and W. M. Sachtler, *Catal. Today*, 1998, **42**, 73-83.
21. K. Fajerwerg and H. Debellefontaine, *Appl. Catal. B: Environ.*, 1996, **10**, L229-L235.
22. K. Fajerwerg, J. N. Foussard, A. Perrard and H. Debellefontaine, *Water Sci. Technol.*, 1997, **35**, 103-110.
23. N. H. Phu, T. T. K. Hoa, N. Van Tan, H. V. Thang and P. Le Ha, *Appl. Catal. B: Environ.*, 2001, **34**, 267-275.
24. M. M. Treacy and J. B. Higgins, *Collection of Simulated XRD Powder Patterns for Zeolites Fifth (5th) Revised Edition*. Elsevier: 2007.
25. S. Chaliha and K. G. Bhattacharyya, *Chem. Eng. J.*, 2008, **139**, 575-588.
26. S. Chaliha and K. G. Bhattacharyya, *J. Hazard. Mater.*, 2008, **150**, 728-736.
27. P. L. Tan, Y. L. Leung, S. Y. Lai and C. T. Au, *Appl. Catal. A: Gen.*, 2002, **228**, 115-125.
28. D. Scarano, A. Zeccdhine, S. Bordiga, F. Geobaldo and G. Spoto, *J. Chem. Soc., Faraday Trans*, 1993, **89**, 4123-4130.
29. R. Szoztak, *Blackie Academic and Professional, London*, 1998, **359**.
30. S. Bordiga, R. Buzzoni, F. Geobaldo, C. Lamberti, E. Giamello, A. Zecchina, G. Leofanti, G. Petrini, G. Tozzola and G. Vlaic, *J. Catal.*, 1996, **158**, 486-501.
31. A. Ates, A. Reitzmann and G. Waters, *Appl. Catal. B: Environ.*, 2012, **119 – 120**, 329-339.
32. D. Meloni, R. Monaci, V. Solinas, G. Berlier, S. Bordiga, I. Rossetti, C. Oliva and L. Forni, *J. Catal.*, 2003, **214**, 169-178.
33. E. Dumitriu, V. Hulea, I. Fechete, A. Auroux, J. Lacaze and C. Guimon, *Micropor. Mesopor. Mat.*, 2001, **43**, 341-359.

View Article Online
DOI: 10.1039/C5RA19832A

34. E. Guélou, J. Barrault, J. Fournier and J. Tatibouët, *Appl. Catal. B: Environ.*, 2003, **44**, 1-8.

35. S. Zhang, X. Zhao, H. Niu, Y. Shi, Y. Cai and G. Jiang, *J. Hazard. Mater.*, 2009, **167**, 560-566.

36. H. R. Eisenhauer, *Journal (Water Pollution Control Federation)*, 1964, 1116-1128.

37. M. Neamtu, C. Zaharia, C. Catrinescu, A. Yediler, M. Macoveanu and A. Kettrup, *Appl. Catal. B: Environ.*, 2004, **48**, 287-294.

38. J. A. Zazo, J. A. Casas, A. F. Mohedano and J. J. Rodriguez, *Appl. Catal. B: Environ.*, 2006, **65**, 261-268.

39. F. Adam, J. Andas and I. A. Rahman, *Chem. Eng. J.*, 2010, **165**, 658-667.

40. A. Santos, P. Yustos, A. Quintanilla, F. Garcia-Ochoa, J. A. Casas and J. J. Rodriguez, *Environ. Sci. Technol.*, 2004, **38**, 133-138.

41. G. Centi, S. Perathoner, T. Torre and M. G. Verduna, *Catal. Today*, 2000, **55**, 61-69.

42. M. Dükkancı, G. Gündüz, S. Yılmaz and R. V. Prihod Ko, *J. Hazard. Mater.*, 2010, **181**, 343-350.

43. T. D. Nguyen, N. H. Phan, M. H. Do and K. T. Ngo, *J. Hazard. Mater.*, 2011, **185**, 653-661.

44. M. Pera-Titus, V. Garcı´a-Molina, M. A. Baños, J. Giménez and S. Esplugas, *Appl. Catal. B: Environ.*, 2004, **47**, 219-256.

45. H. Xu, D. Zhang and W. Xu, *J. Hazard. Mater.*, 2008, **158**, 445-453.

View Article Online
DOI: 10.1039/C5RA19832A

Figure content:

Fig. 1. XRD patterns of different samples: (a) ZSM-5, (b) Fe_2O_3/ZSM-5 and (c) Fe-ZSM-5.

Fig. 2. IR spectra of different samples: (a) ZSM-5, (b) Fe_2O_3/ ZSM-5 and (c) Fe-ZSM-5.

Fig. 3. H_2-TPR profiles of different samples: (a) Fe-ZSM-5, (b) ZSM-5.

Fig. 4. UV-vis reflectance spectrum of Fe-ZSM-5.

Fig. 5. Effect of reaction temperature on phenol conversion with Fe-ZSM-5 ($[phenol]_0$: 2500 mg/L, $[H_2O_2]_0$: 19000 mg/L, catalyst concentration=2.5 g/L, pH=4, stirring rate=400 rpm).

Fig. 6. Effect of pH on phenol conversion with Fe-ZSM-5 ($[phenol]_0$: 2500 mg/L, $[H_2O_2]_0$: 19000 mg/L, catalyst concentration=2.5 g/L, *T*=70 ℃, stirring rate=400 rpm).

Fig. 7. Effect of catalyst concentration on phenol conversion with Fe-ZSM-5 ($[phenol]_0$: 2500 mg/L, $[H_2O_2]_0$: 19000 mg/L, pH=4, *T*=70 ℃, stirring rate=400 rpm).

Fig. 8. Effect of stirring rate on phenol conversion with Fe-ZSM-5 ($[phenol]_0$: 2500 mg/L, $[H_2O_2]_0$: 19000 mg/L, catalyst concentration=2.5 g/L, pH=4, *T*=70 ℃).

Fig. 9. Conversion of phenol with Fe-ZSM-5 and Fe_2O_3/ZSM-5 ($[phenol]_0$: 2500 mg/L, $[H_2O_2]_0$: 19000 mg/L, catalyst concentration=2.5 g/L, pH=4, *T*=70 ℃, stirring rate =400 rpm).

Fig. 10. Selectivity to CO_2 with Fe-ZSM-5 and Fe_2O_3/ZSM-5 ($[phenol]_0$: 2500 mg/L, $[H_2O_2]_0$: 19000 mg/L, catalyst concentration=2.5 g/L, pH=4, *T*=70 ℃, stirring rate =400 rpm).

Fig. 11. Distribution curves of identified aromatics intermediates in the oxidation of phenol: (a) Fe-ZSM-5, (b) Fe_2O_3/ZSM-5 ($[phenol]_0$: 2500 mg/L, $[H_2O_2]_0$: 19000 mg/L, catalyst concentration=2.5 g/L, pH=4, *T*=70 ℃, stirring rate = 400 rpm).

Fig. 12. Fe leached in the oxidation of phenol over Fe-ZSM-5 and Fe_2O_3/ZSM-5 ($[phenol]_0$: 2500 mg/L, $[H_2O_2]_0$: 19000 mg/L, catalyst concentration=2.5 g/L, pH=4, *T*=70 ℃, stirring rate =400 rpm).

Fig. 13. Reusability of Fe-ZSM-5 under optimum reaction conditions.

Fig. 14. Effect of stirring rate on initial rate of phenol ($[phenol]_0$: 2500 mg/L, $[H_2O_2]_0$: 19000 mg/L, catalyst concentration=2.5 g/L, pH=4, *T*=70 ℃).

Fig. 15. Effect of particle size of catalyst on initial rate of phenol ($[phenol]_0$: 2500 mg/L, $[H_2O_2]_0$: 19000 mg/L, catalyst concentration=2.5 g/L, pH=4, *T*=70 ℃).

Fig. 16. First-order oxidation of phenol by catalytic wet oxidation over Fe-ZSM-5 ($[phenol]_0$: 2500 mg/L, $[H_2O_2]_0$:

View Article Online
DOI: 10.1039/C5RA19832A

19000 mg/L, catalyst concentration=2.5 g/L, pH=4, stirring rate=400 rpm, particle size: 80 meshes).

Fig. 17. Arrhenius plot of ln *k* vs.*1/T*.

View Article Online
DOI: 10.1039/C5RA19832A

Fig. 1. XRD patterns of different samples: (a) ZSM-5, (b) Fe_2O_3/ZSM-5 and (c) Fe-ZSM-5.

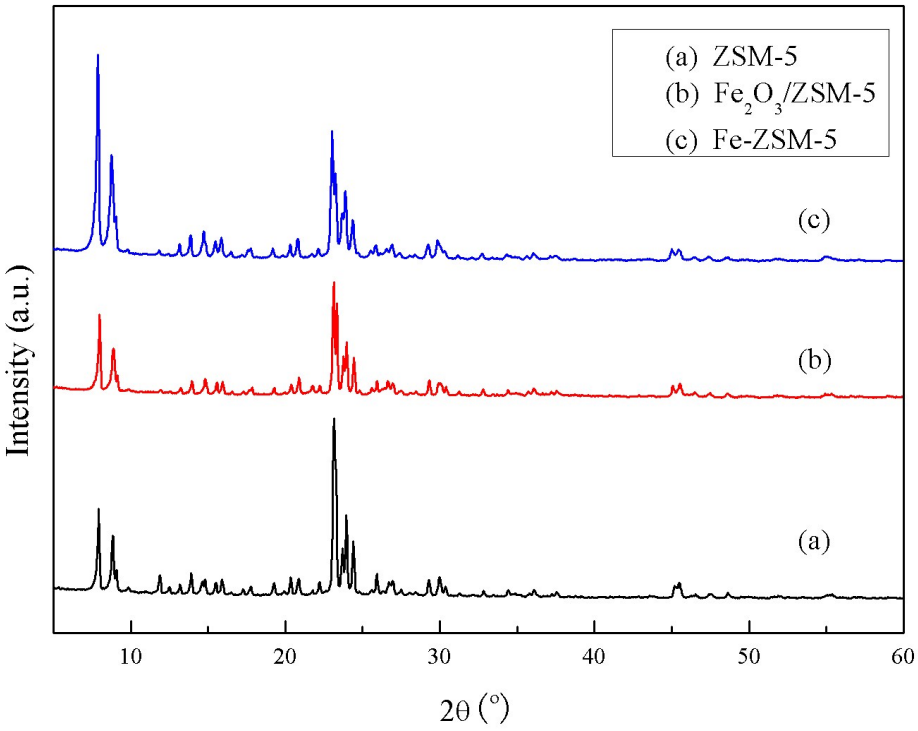

View Article Online
DOI: 10.1039/C5RA19832A

Fig. 2. IR spectra of different samples: (a) ZSM-5, (b) Fe_2O_3/ ZSM-5 and (c) Fe-ZSM-5.

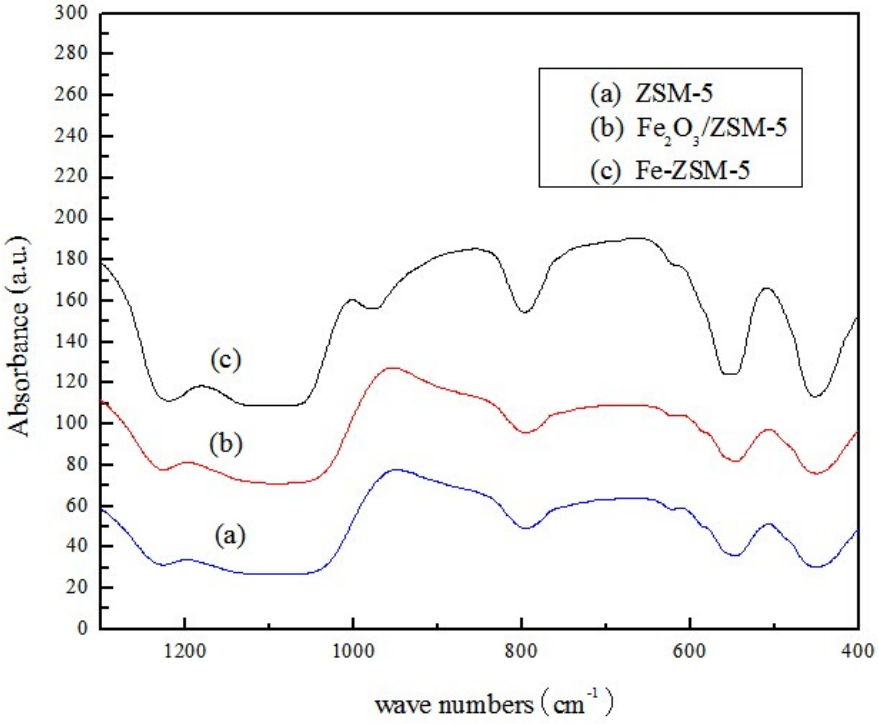

View Article Online
DOI: 10.1039/C5RA19832A

Fig. 3. H_2-TPR profiles of different samples: (a) Fe-ZSM-5, (b) ZSM-5.

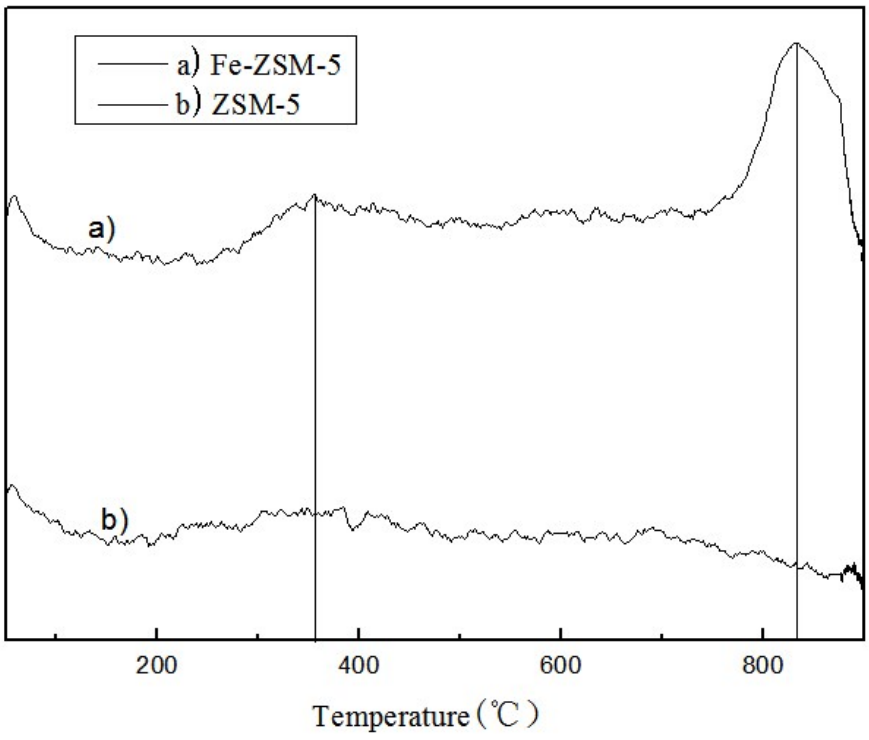

View Article Online
DOI: 10.1039/C5RA19832A

Fig. 4. UV-vis reflectance spectrum of Fe-ZSM-5.

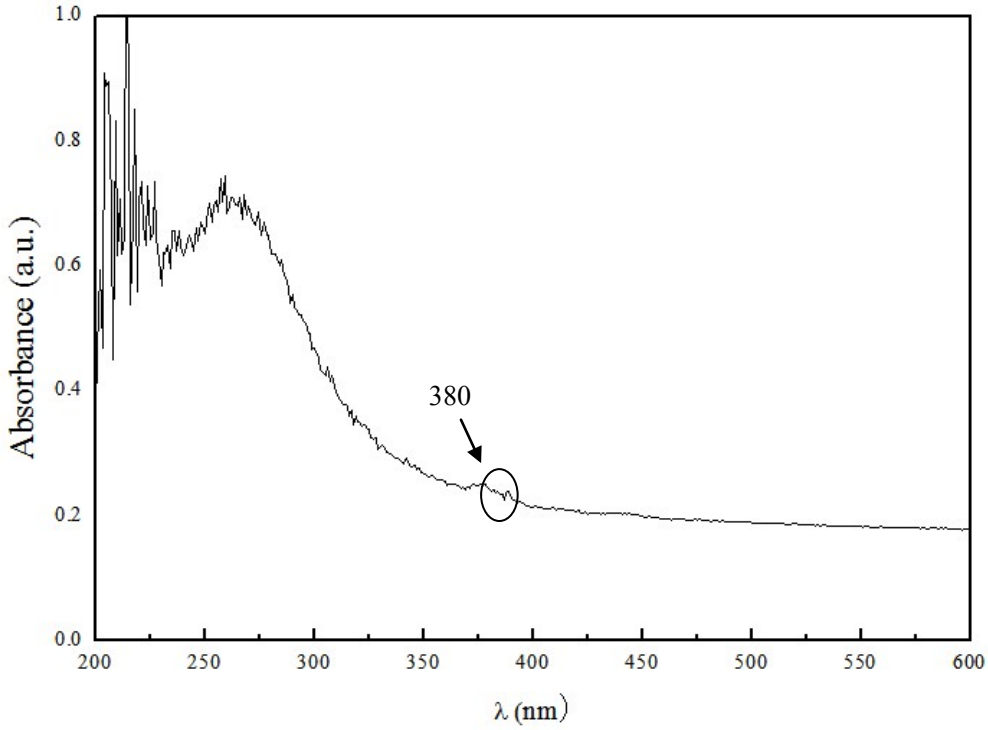

View Article Online
DOI: 10.1039/C5RA19832A

Fig. 5. Effect of reaction temperature on phenol conversion with Fe-ZSM-5 ([phenol]$_0$: 2500 mg/L, [H_2O_2]$_0$: 19000 mg/L, catalyst concentration=2.5 g/L, pH=4, stirring rate=400 rpm).

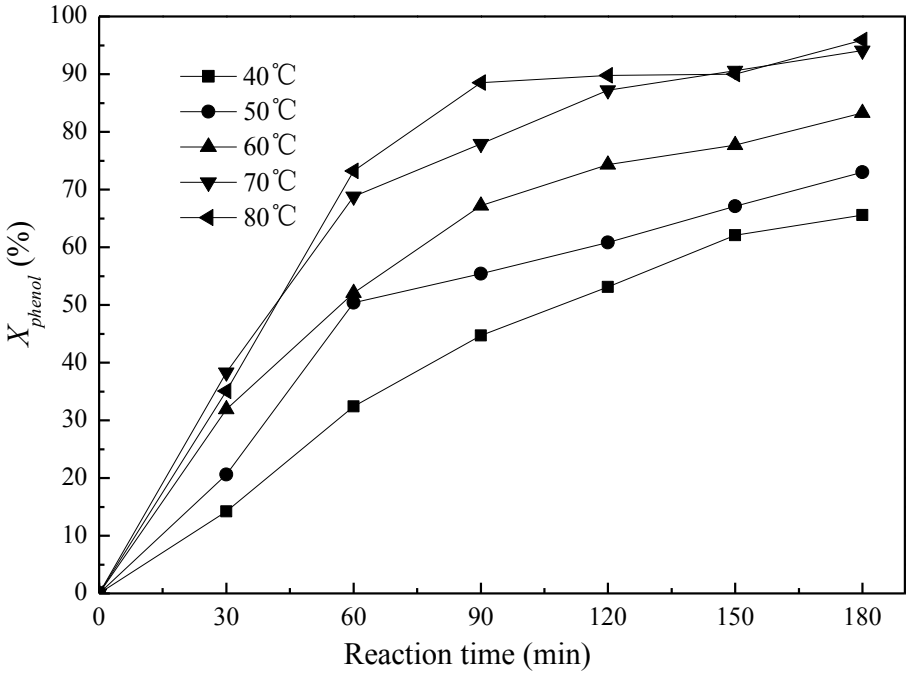

View Article Online
DOI: 10.1039/C5RA19832A

Fig. 6. Effect of pH on phenol conversion with Fe-ZSM-5 ([phenol]$_0$: 2500 mg/L, [H_2O_2]$_0$: 19000 mg/L, catalyst concentration=2.5 g/L, *T*=70 ℃, stirring rate=400 rpm).

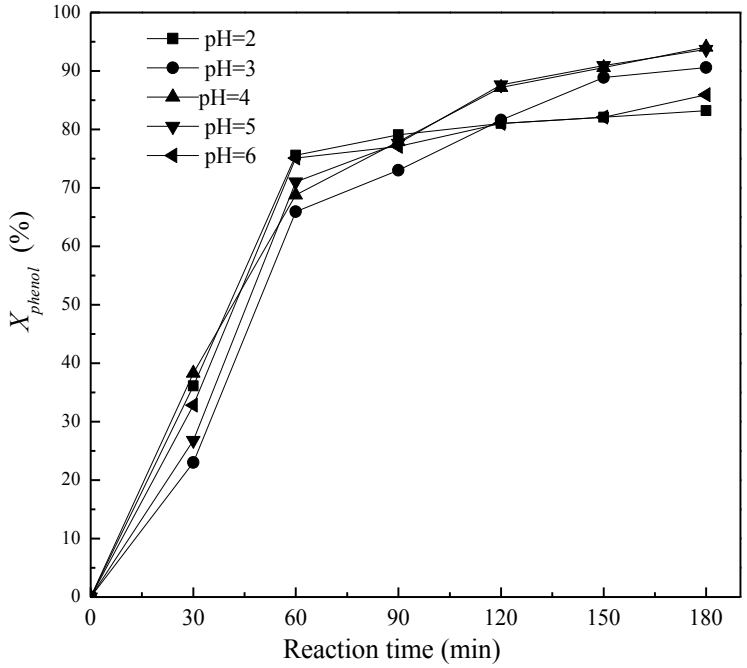

(a)

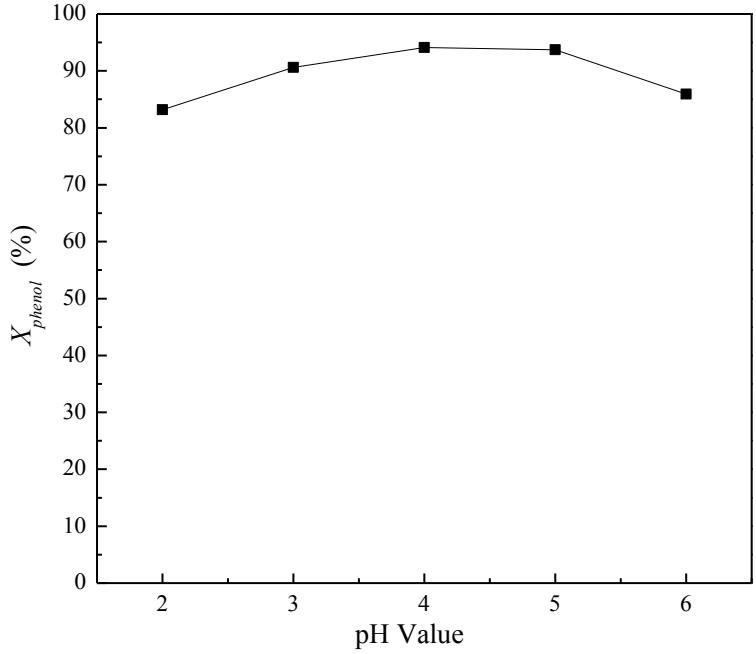

(b)

View Article Online
DOI: 10.1039/C5RA19832A

Fig. 7. Effect of catalyst concentration on phenol conversion with Fe-ZSM-5 ([phenol]$_0$: 2500 mg/L, [H_2O_2]$_0$: 19000 mg/L, pH=4, *T*=70 ℃, stirring rate=400 rpm).

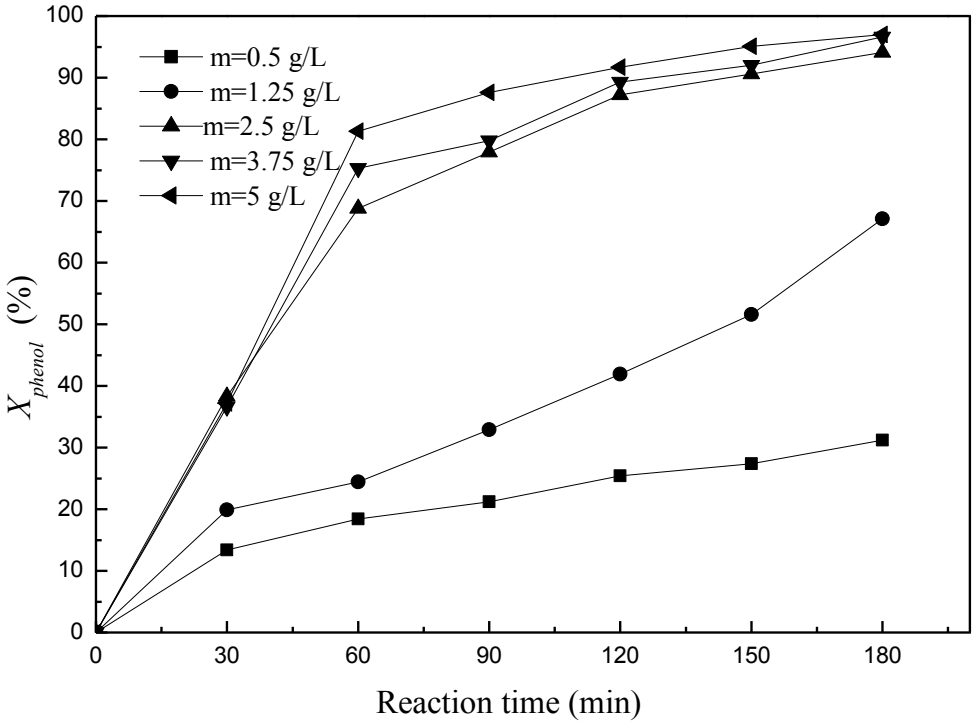

View Article Online
DOI: 10.1039/C5RA19832A

Fig. 8. Effect of stirring rate on phenol conversion with Fe-ZSM-5 ([phenol]$_0$: 2500 mg/L, [H_2O_2]$_0$: 19000 mg/L, catalyst concentration=2.5 g/L, pH=4, *T*=70 ℃).

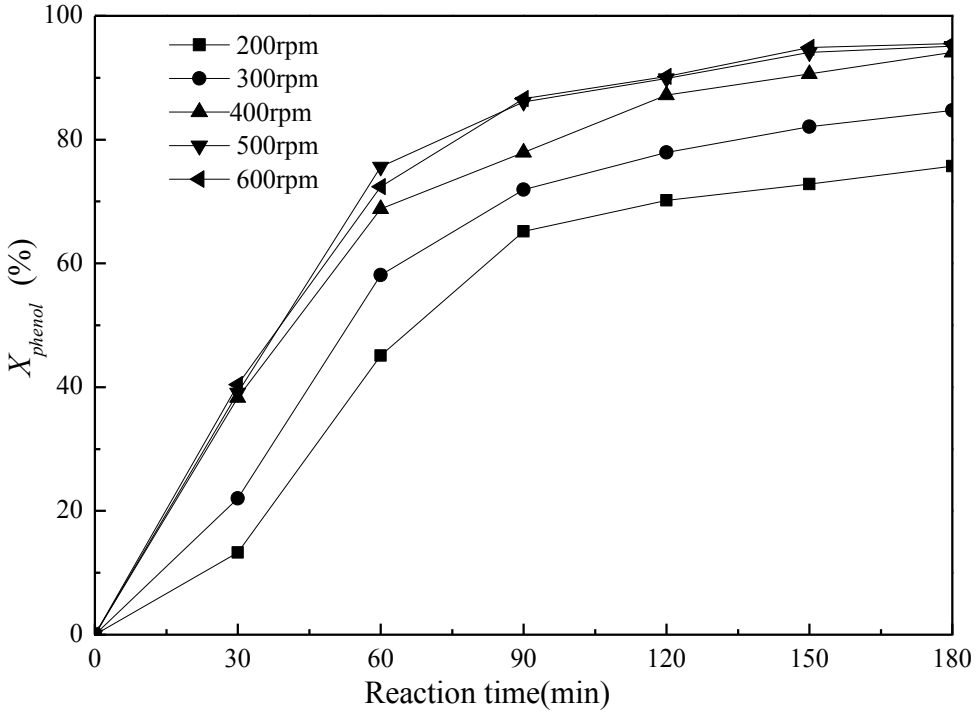

View Article Online
DOI: 10.1039/C5RA19832A

Fig. 9. Conversion of phenol with Fe-ZSM-5 and Fe_2O_3/ZSM-5 ($[phenol]_0$: 2500 mg/L, $[H_2O_2]_0$: 19000 mg/L, catalyst concentration=2.5 g/L, pH=4, T=70 ℃, stirring rate =400 rpm).

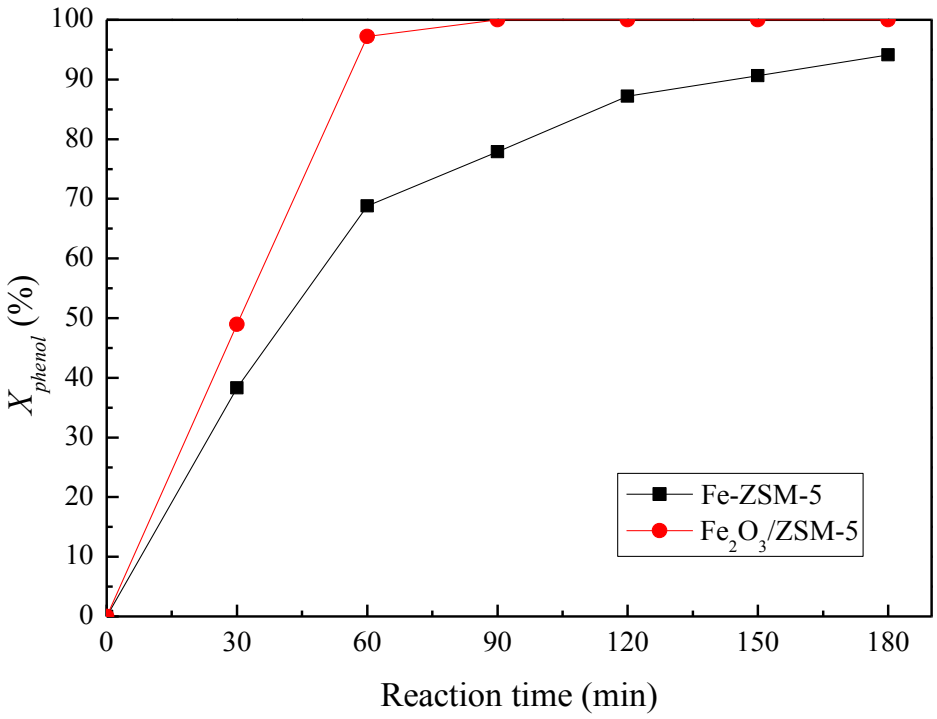

View Article Online
DOI: 10.1039/C5RA19832A

Fig.10. Selectivity to CO_2 with Fe-ZSM-5 and Fe_2O_3/ZSM-5 ([phenol]$_0$: 2500 mg/L, [H_2O_2]$_0$: 19000 mg/L, catalyst concentration=2.5 g/L, pH=4, T=70 ℃, stirring rate =400 rpm).

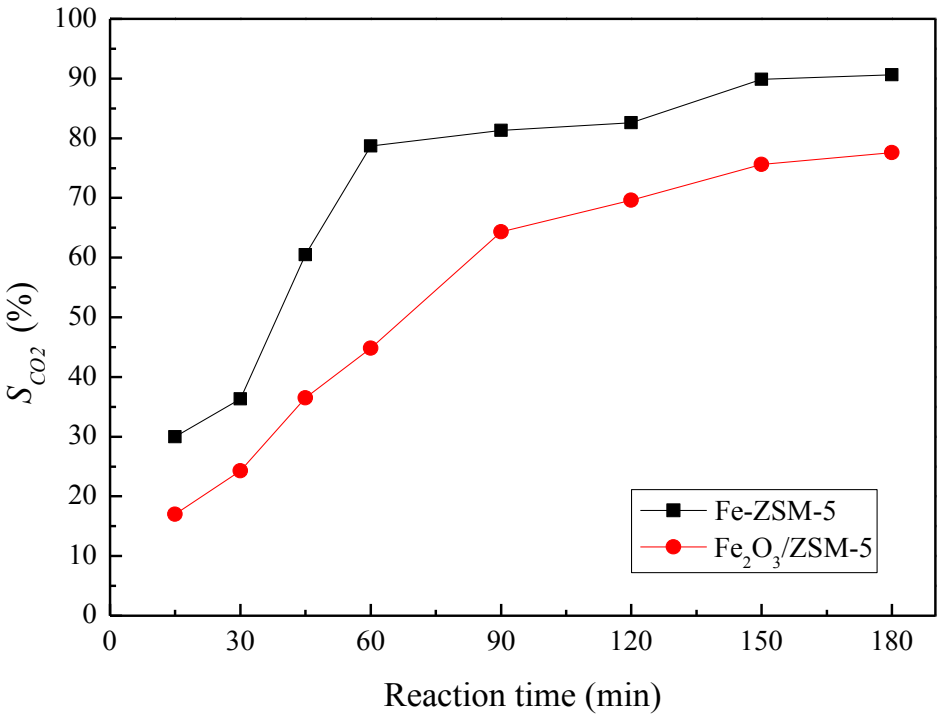

View Article Online
DOI: 10.1039/C5RA19832A

Fig. 11. Distribution curves of identified aromatics intermediates in the oxidation of phenol: (a) Fe-ZSM-5, (b) Fe_2O_3/ZSM-5 ([phenol]$_0$: 2500 mg/L, [H_2O_2]$_0$: 19000 mg/L, catalyst concentration=2.5 g/L, pH=4, *T*=70 ℃, stirring rate = 400 rpm).

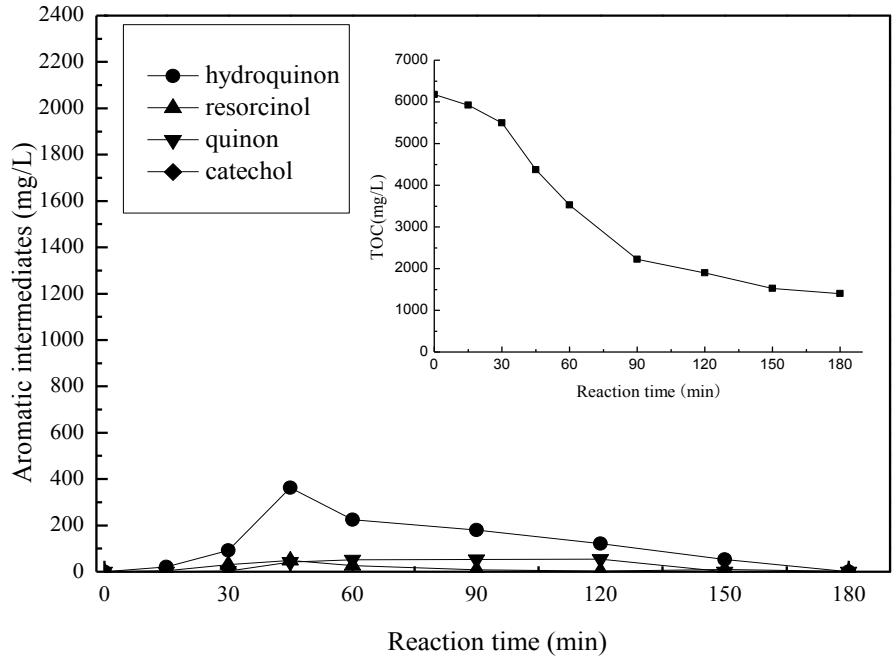

(a)

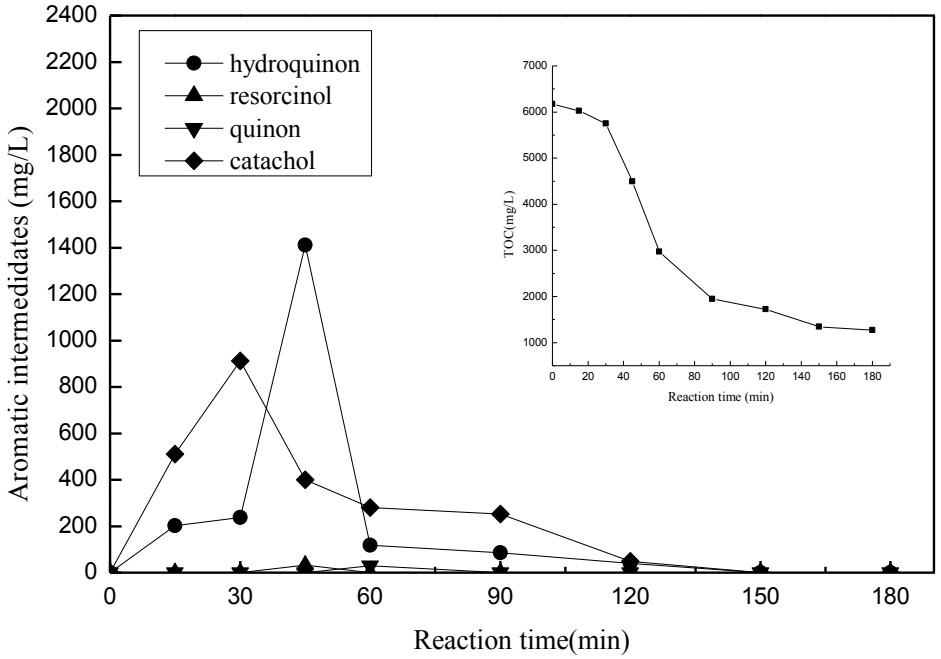

(b)

View Article Online
DOI: 10.1039/C5RA19832A

Fig. 12. Fe leached in the oxidation of phenol over Fe-ZSM-5 and Fe_2O_3/ZSM-5 ([phenol]$_0$: 2500 mg/L, [H_2O_2]$_0$: 19000 mg/L, catalyst concentration=2.5 g/L, pH=4, *T*=70 ℃, stirring rate =400 rpm).

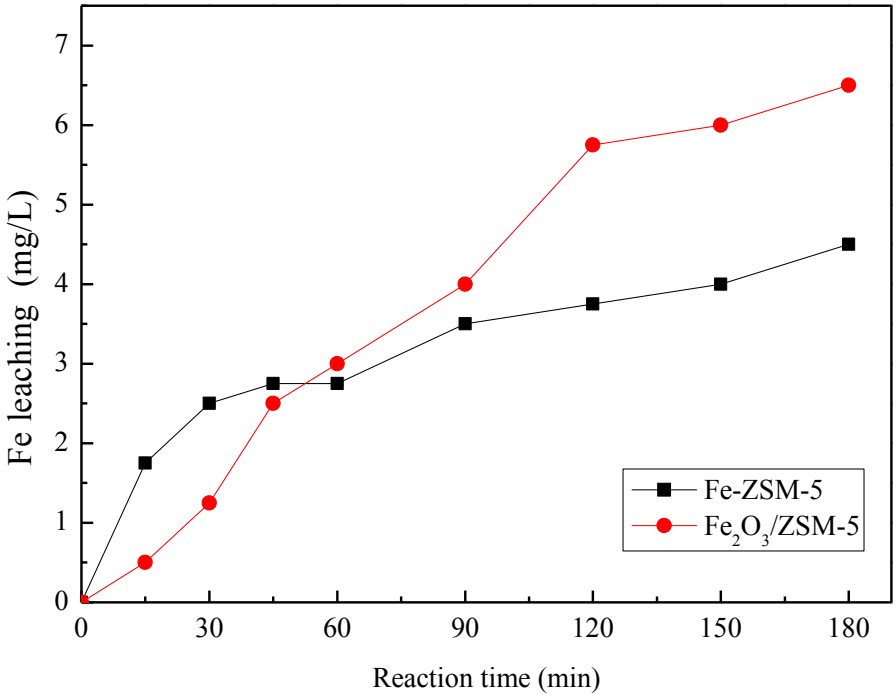

View Article Online
DOI: 10.1039/C5RA19832A

Fig. 13. Reusability of Fe-ZSM-5 under optimum reaction conditions.

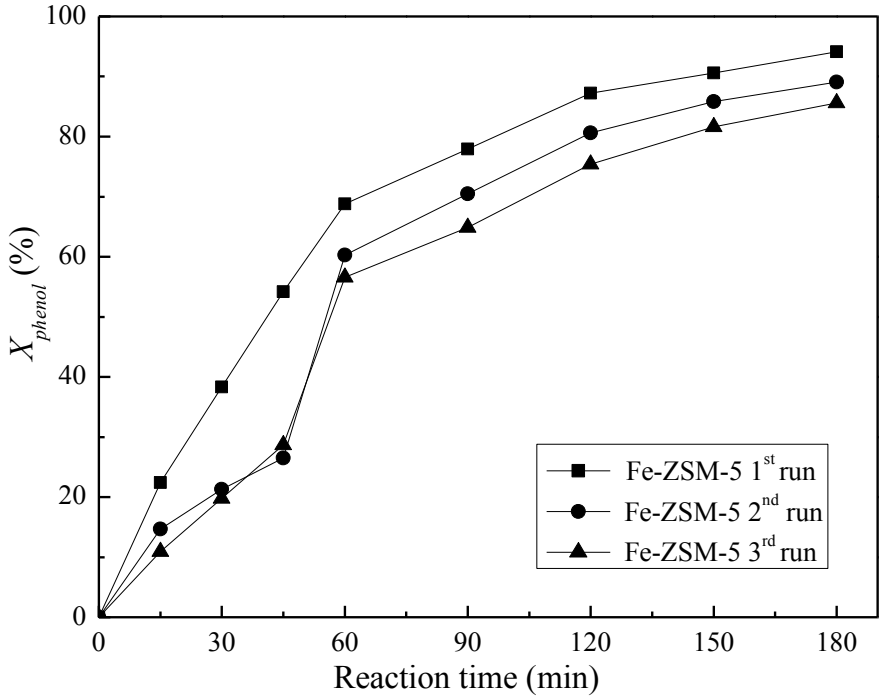

View Article Online
DOI: 10.1039/C5RA19832A

Fig. 14. Effect of stirring rate on initial rate of phenol ([phenol]$_0$: 2500 mg/L, [H_2O_2]$_0$: 19000 mg/L, catalyst concentration=2.5 g/L, pH=4, *T*=70 ℃).

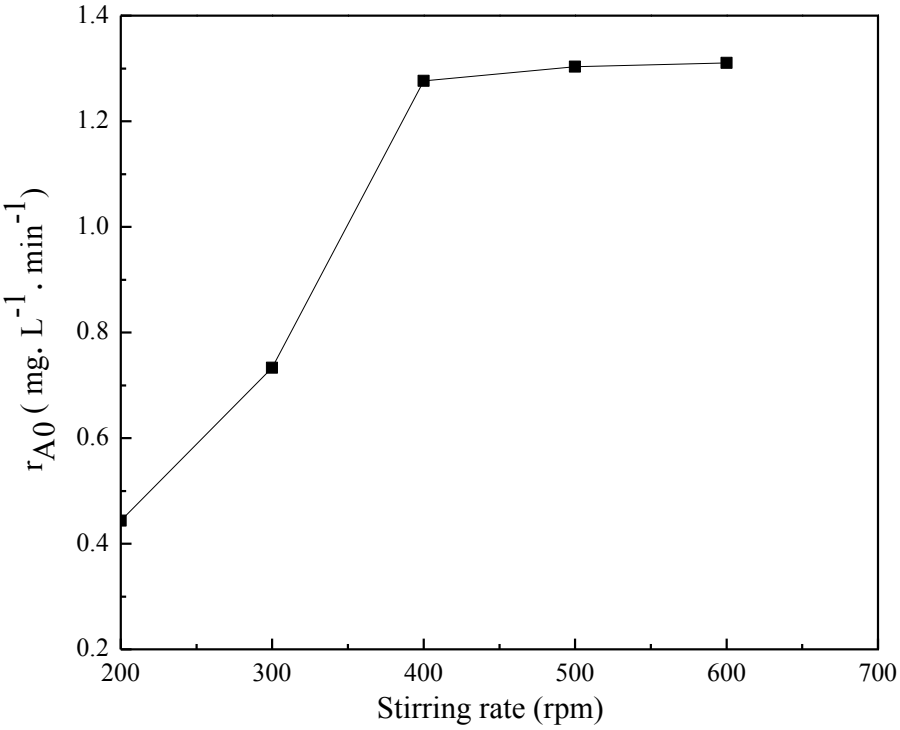

View Article Online
DOI: 10.1039/C5RA19832A

Fig. 15. Effect of particle size of catalyst on initial rate of phenol ([phenol]$_0$: 2500 mg/L, [H_2O_2]$_0$: 19000 mg/L, catalyst concentration=2.5 g/L, pH=4, *T*=70 ℃).

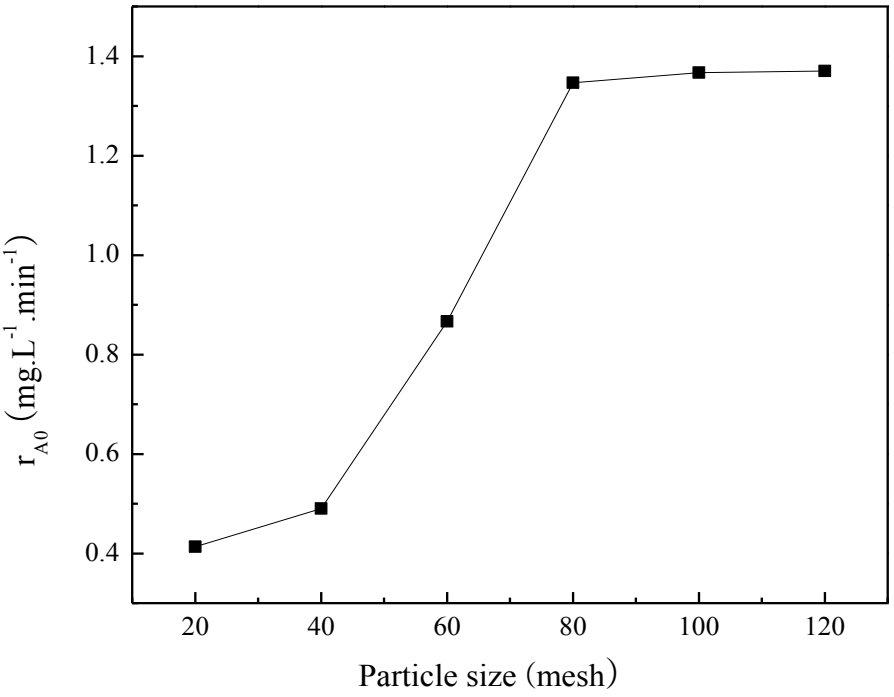

View Article Online
DOI: 10.1039/C5RA19832A

Fig. 16. First-order oxidation of phenol by catalytic wet oxidation over Fe-ZSM-5 ([phenol]$_0$: 2500 mg/L, [H_2O_2]$_0$: 19000 mg/L, catalyst concentration=2.5 g/L, pH=4, stirring rate=400 rpm, particle size: 80 meshes).

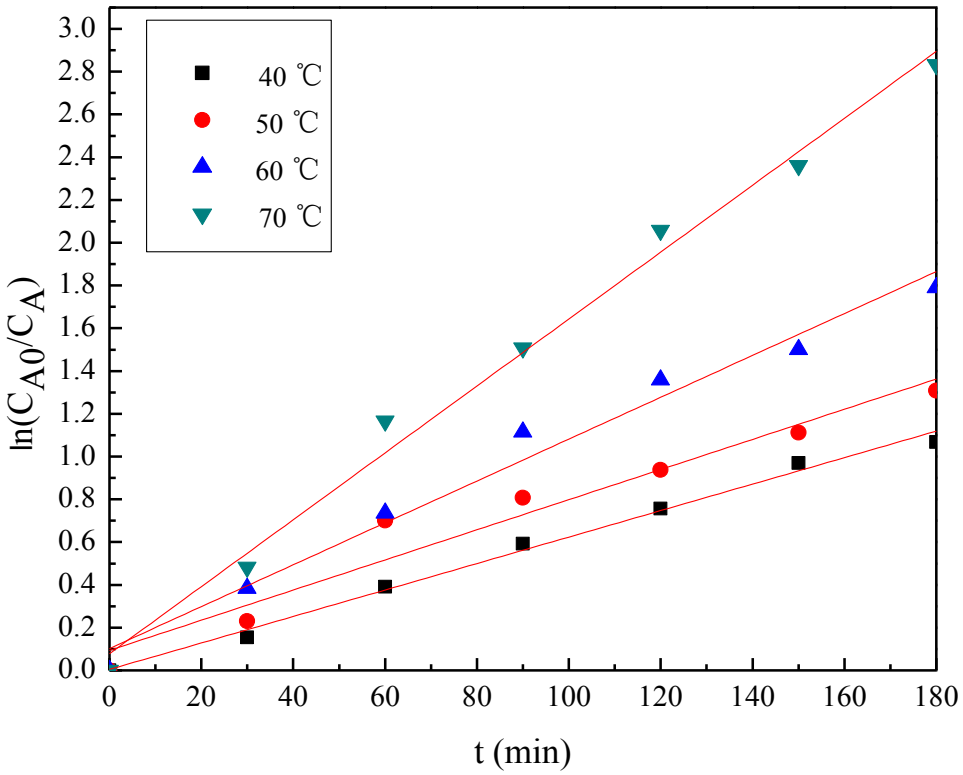

View Article Online
DOI: 10.1039/C5RA19832A

Fig. 17. Arrhenius plot of ln *k* vs.*1/T*.

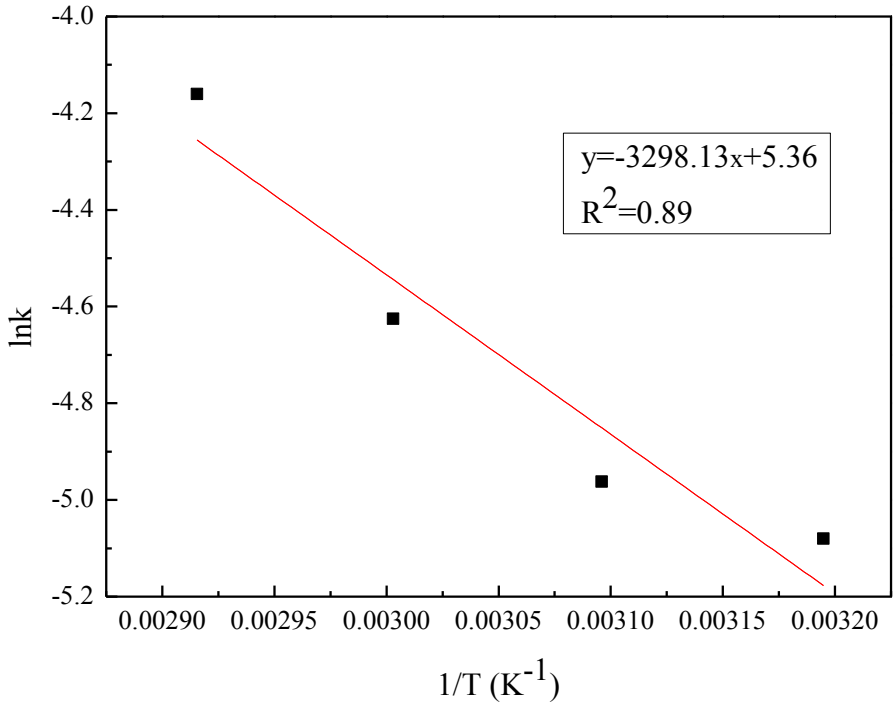

View Article Online
DOI: 10.1039/C5RA19832A

Graphical Abstract:

Systematically study of catalytic wet oxidation of phenol over Fe-ZSM-5 and Fe_2O_3/ZSM-5 catalysts.